Electronic Conductance Behavior of Carbon-Based Molecular Junctions with Conjugated Structures

Franklin Anariba and Richard L. McCreery*

Department of Chemistry, The Ohio State University, 100 West 18th Avenue, Columbus, Ohio 43210-1185

Received: June 11, 2002; In Final Form: July 25, 2002

A novel molecular junction based on a monolayer between carbon and mercury "contacts" was investigated by examining current/voltage behavior as a function of temperature and monolayer thickness. Monolayers of phenyl, biphenyl, and terphenyl were covalently bonded to flat, graphitic carbon, then a top contact was formed with a suspended mercury drop. Similar molecular junctions were formed from multilayer nitroazobenzene (NAB) films of 30 Å and 47 Å thickness, and junctions were examined over the temperature range of +80 °C to −50 °C. Junction resistances were a strong function of molecular length and structure, with mean resistances for 0.78 mm^2 junctions of 34.4 Ω, 13.8 KΩ, and 41.0 KΩ for phenyl, biphenyl, and terphenyl junctions. The *i*/*V* characteristics of biphenyl and phenyl junctions were nearly independent of temperature, while those of terphenyl and NAB junctions were temperature independent below 0 °C but thermally activated above 10 °C. The results are consistent with a tunneling process at low temperature, where the molecular conformations are apparently fixed. For the thicker terphenyl and NAB junctions, the tunneling rate is sufficiently slow to observe a thermally activated conduction process at higher temperatures. The observed activation barriers of 0.3 to 0.8 eV are in the range expected for phenyl ring rotation, implying that the coplanar conformer of terphenyl has a significantly higher conductivity. Below 0 °C, the junction is presumably "frozen", with only a small fraction of terphenyl molecules in the conductive conformation. Calculated HOMO-LUMO gaps for the planar and twisted conformations of terphenyl predict that the planar geometry is five times more conductive than the twisted conformation. In addition to presenting a new type of molecular electronic junction, the results bear on the widespread topic of electronic conductivity of organic molecules.

Introduction

The concept of a molecular junction has been recognized for some time, as a subset of the more general area of molecular electronics. Molecular junctions reported to date vary significantly in size, number of molecules, and the nature of the electrical contacts, but they all share one core principle. A single molecule or collection of parallel molecules is oriented between two electronic conductors, such that molecular properties affect or control electron flow through the junction. An important feature of molecular junctions is the prospect of creating a wide variety of current/voltage (*i*/*V*) characteristics by structural changes in the molecule. Since molecules can exhibit a wide range of molecular orbital patterns, there should be a corresponding wide range of *i*/*V* transfer functions. A second important motive for studying molecular junctions is elucidation of the electron transport mechanisms which underlie molecular electronics.[1,2] It is obvious that the creation of molecular circuits in which molecular structure is used to control conductivity will require knowledge of electron transport mechanisms. Molecular junctions provide direct control of applied voltage and observed current, and are a simple alternative to electron transport examined by electrochemical and photochemical techniques.

While a variety of molecular junctions involve multilayer films of redox or conducting polymers, the types of greatest relevance to the current work are based on organic monolayers between electronic conductors. Langmuir Blodgett (L-B) or Au/thiol self-assembled monolayers (SAMs) have been oriented between metallic conductors (e.g., Au, Ag, Hg, Ti) to make a variety of molecular junctions involving a few molecules or a much larger assembly. Such junctions have exhibited a variety of interesting effects, including Coulomb staircases,[3−5] Schottky barriers,[6,7] rectification,[8,9] charge storage,[10] and staircase current/voltage curves.[11] The *i*/*V* characteristics of these molecular junctions have stimulated a large theoretical effort to explain their electronic behavior, as well as numerous discussions and patents regarding potential practical applications. To date the rapid increase of interest in molecular junctions has been based on either SAM or L-B approaches involving a variety of junction designs, ranging from junctions containing a few active molecules[6,8,12,13] to Hg-based junctions with areas approaching 1 mm^2 and containing $>10^9$ molecules.[14−16]

Although molecular junctions based on L-B and SAM structures have revealed important properties of electron transport, they present some barriers to implementation in practical devices. L-B films are fragile, and junction fabrication is generally a delicate process with possibly large variations in yield. Both L-B and SAM junctions have significant energy barriers at the interface between the monolayer and the contacts. For example, the gold−sulfur bond common in SAMs presents a ∼2 eV energy barrier which must be overcome to initiate electronic conduction.[3,7,12] The domain size in Au/thiol SAMs is generally limited to areas of $\ll 1\ \mu m^2$, thus preventing fabrication of any but very small defect-free junctions.

A large body of literature exists on the mechanism of charge transport through monolayers in electrochemical interfaces (conductor/monolayer/solution)[17−21] and molecular junctions

* Corresponding author. E-mail: mccreery.2@osu.edu.

10.1021/jp026285e CCC: $22.00
Published on Web 09/05/2002

TABLE 1: Conduction Mechanisms in Metal/Dielectric/Metal Thin Film Junctions[a]

	temperature (T) dependence	voltage (V) dependence	monolayer thickness (d) dependence
coherent, nonresonant tunneling	weak	linear (low V)	$\exp(-\beta d)$
coherent, resonant tunneling	weak	linear	weak
incoherent, diffusive tunneling "tight binding model"	weak	linear (low V)	see note (b)
field emission (high E-field, "Fowler Nordheim")	weak	$V^2 \exp(-b_1/V)$[c]	$\exp(-c_2 d)$
thermionic (Schottky) emission	$\exp(-a_1/T)$	$\exp(b_2 V^{1/2})$	$\exp(-c_3 d^{1/2})$
"hopping"	$\exp(-a_2/T)$	linear (low V)	d^{-1}
Poole Frenkel effect ("traps")	$\exp(-a_3/T)$	$\exp(b_3 V^{1/2})$	$\exp(-c_4 d^{1/2})$

[a] Adapted from ref 55, p 403, plus refs 1,8,27,56. [b] Depends on choice of parameters, see ref 27. [c] a_1, a_2, b_1, etc., refer to constants which do not depend on thickness, temperature, or voltage, but may vary for different conduction mechanisms.

(conductor/molecule/conductor).[3,6−8,14−16,22−26] Several of the mechanisms proposed for electron conduction through such systems are listed in Table 1, along with the expected temperature (T), voltage (V), and thickness (d) dependencies. Nonresonant tunneling is the classical case in which all of the energy levels in the monolayer molecule differ significantly in energy from the Fermi levels of the conductors, while resonant tunneling requires a molecular orbital close to the conductor Fermi level. The tight binding model refers to electron (or hole) motion between a series of sites, via a sequence of tunneling events through the energy barriers between adjacent sites.[27] Field emission refers to assistance of tunneling by an electric field, in which the tunneling probability increases nonlinearly with voltage. All four tunneling mechanisms are independent of temperature, at least in their simplest forms. However, they vary significantly in the predicted shape of their current/voltage (i/V) characteristics and their variation with monolayer thickness.

The remaining conduction mechanisms listed in Table 1 involve thermal activation of an electron over a barrier, and hence are exponentially dependent on temperature. Thermionic emission may occur upon injection of an electron from a conductor into a molecular monolayer. The applied field lowers the activation barrier, resulting in a dependence on both V and d. "Hopping" consists of thermally activated electron transfer between sites in the monolayer, and yields essentially ohmic behavior at a given temperature, often with a d^{-1} dependence.[6,28−30] Poole-Frenkel transmission involves thermal activation of electrons out of Coulombic "traps" which may be present as defects in the monolayer. Electron transmission occurs when the applied field and temperature are sufficient to permit electrons to leave a "trap". Since the various mechanisms for charge transport through monolayers are numerous, it is generally necessary to examine conductivity as a function of T, V, and d to narrow down the possibilities.

In a recent letter,[16] we described a fundamentally novel molecular junction structure based on organic monolayers covalently bonded to a graphitic carbon substrate, as shown in Figure 1. Since monolayer bonding to the carbon "contact" involves a phenyl ring conjugated to the graphitic π system, we expect a low energy barrier to electron transfer between the carbon substrate and the monolayer. A mercury drop provides the second contact, and permits investigation of the i/V characteristics of the junction. Once the junction is formed, it contains no intentional electrolyte or solution, and may be examined over a wide temperature range (at least +80 °C to −50 °C). Like the Hg/molecule/Hg and Hg/molecule/Ag junctions reported using thiol chemistry,[14,15] the junctions are relatively simple to produce and a wide range of molecules may be examined. The current report describes carbon-based molecular junctions in more detail, with emphasis on the effect of monolayer structure and temperature on electron transport through the junction.

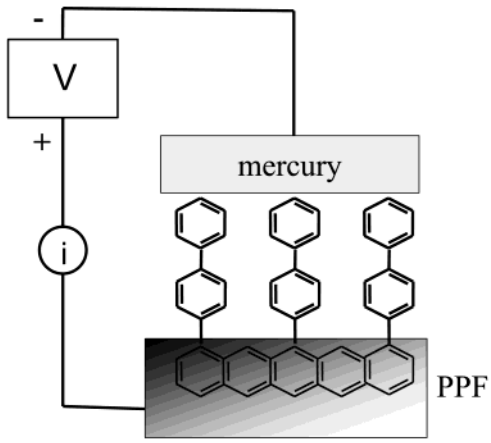

Figure 1. Schematic of carbon-based molecular junction using a biphenyl monolayer. Aromatic rings in pyrolyzed photoresist film (PPF) represent the graphitic B system of the carbon support.

Experimental Section

Phenyl, biphenyl, terphenyl, and 4-nitroazobenzene (NAB) diazonium tetrafluoroborate salts were prepared from their respective amines using established procedures.[31−34] The salts were stored in a freezer in the dark and were used within one month of synthesis. Pyrolyzed photoresist films (PPF) were prepared on polished glassy carbon substrates as described previously.[35,36] Care was taken to reduce trace oxygen in the pyrolysis atmosphere, and pyrolyzed samples were inspected in a light microscope for evidence of porosity or defects. Specimens with a low density of visible defects were cleaned with 50/50 isopropanol (IPA)/acetonitrile which had been purified with activated carbon before electrochemical derivatization.[37] Phenyl, biphenyl, and terphenyl monolayers were prepared by electrochemical reduction of the 1 mM acetonitrile solutions of corresponding diazonium salts containing 0.1 M tetrabutylammonium tetrafluoroborate. The applied potential was scanned at 0.2 V/s for two bi-directional scans from +0.4 to −0.8 V vs Ag/Ag^+. The biphenyl and terphenyl modified surfaces were confirmed to be monolayers with AFM, by observing the depth of an intentional square hole made in the monolayer with the AFM tip. The phenyl monolayer was too thin to observe in this fashion. NAB is prone to forming multilayers, so either 2 or 4 voltammetric scans were used to form films with thicknesses of 30 and 47 Å, respectively.[38] Immediately following derivatization and again before forming a molecular junction, the sample was rinsed with 50/50 IPA/acetonitrile. The sample was then mounted on a copper surface which provided electrical contact, and was itself mounted on a thermoelectric cooling element. With the addition of a resistance heater, the sample temperature was controlled to ±1 °C between +80 and −55 °C.

The mercury top contact was formed in a recessed well made by a ~3 mm section of insulation protruding past the end of a 1.6 mm diameter hook-up wire about 5 cm long. Hg injected into the recess made contact with the metal wire, and formed a hemispherical drop when inverted. Thus the mercury was suspended from the end of the contact wire and within a tube of insulation, and formed a drop with an approximately 1.0 mm diameter. A 3-axis positioner above the sample held the wire, and the entire apparatus (sample, cooler, positioner) was contained in a Plexiglas box with a volume of approximately one cubic foot. The box was purged with dry nitrogen at the start of each experiment, and N_2 flowed continuously for experiments below 20 °C to prevent water condensation. Due to the hazards of heated mercury, THE SAMPLE BOX WAS ACTIVELY VENTED TO A FUME HOOD EXHAUST by a 3-in. diameter hose.

In early experiments, the Hg drop was lowered onto the PPF/monolayer sample with a piezoelectric translator (Burleigh "inchworm") but subsequent experience showed that a manual micrometer was sufficient. The drop was lowered until initial contact with the sample was made, as judged by distortion of the drop visible through an optical magnifier. As the drop was lowered past this point, it deformed, its area increased, and the observed junction resistance decreased by a factor of about 10. Trial and error resulted in a standard procedure for making the Hg contact, under which the drop is lowered 300 μm beyond the initial visual contact. Variation of the initial Hg drop size resulted in a small (~15%) variation in junction area, but visual inspection revealed a junction diameter close to 1 mm and a junction area of 0.78 mm^2. Reproducibility of the low-voltage junction resistance is indicated by Table 2, which lists results from all junctions studied on a total of 12 samples. The "sample number" refers to a distinct preparation carried through the entire pyrolysis and derivatization procedure. Each junction was annealed for 15 h at 20 °C during which low voltage (±0.05 V) resistance measurements were carried out to monitor resistance changes over time. Changes in resistance during this period are discussed in the Results section, and the final resistance values are reported in Table 2. Although the standard deviation of the final resistance was fairly high (~50%), the differences between the means of junctions of different molecules was much larger.

A series of voltammograms was obtained for annealed junctions over a range of temperatures, usually +50 to −55 °C. Reversibility was checked by returning the junction to its initial temperature (usually +50 °C). Although the junction resistance usually changed by 10−20% during a temperature cycle, the observed trends were reproducible.

Results

A current vs voltage plot for a biphenyl junction is shown in Figure 2. For potentials within the range of ±0.5 V, the *i*/*V* characteristic was reversible with no significant hysteresis, and the curve shape and magnitude were independent of voltage scan rate for the range 0.01 V/s to 1000 V/s. At 10,000 V/sec a capacitive current component was observed, but was difficult to measure reliably above the much larger resistive current. The sharp increase in current at ~1.6 V apparent in Figure 2 was irreversible, and its potential varied for different junctions, by approximately ±0.5 V. The *i*/*V* characteristic was linear over a small range near zero volts, corresponding to a junction resistance of 9.9 KΩ in this case. After the apparent breakdown at ~1.6 V, the low voltage resistance irreversibly decreased to <10 Ω. In control experiments including all fabrication steps but absent the diazonium reagent, the observed junction resistance was less than 2 Ω. The most likely explanation for the sharp increase in current at +1.6 V is dielectric breakdown, apparently resulting in a catastrophic failure of the junction. Based on the biphenyl monolayer thickness of 11.1 Å (measured from the PPF carbon surface atom to the van der Waals radius of the opposite hydrogen), the electric field at 1.6 V is >10^7 V/cm.

Current/voltage curves for phenyl, biphenyl, and terphenyl junctions are shown in Figure 3 for applied voltages which avoid

TABLE 2: Observed Resistance ($V = \pm 50$ mV) for Hg-Monolayer-PPF Junctions at 20 °C

monolayer	sample no.	observed junction resistance, Ω
phenyl	1[a]	2[b]
	1	44.3
	1	19.8
	1	18.8
	2	66.7
	2	15.4
	3	26.9
	4	49.0
		mean: 34.4 ± 19
biphenyl	1	9070
	1	16007
	1	14098
	1	6081
	2	27910
	2	9934
	2	11911
	3	16447
		mean: 13800 ± 6200
terphenyl	1	360691[b]
	1	30393
	1	29471
	2	175104[b]
	2	50798
	3	27763
	3	30532
	3	28186
	3	19236
	4	66700
	5	94066
	5	24030
	5	70153
		mean: 41000 ± 23900

[a] Sample number refers to separate preparations of PPF and monolayer. Repeated entries with the same sample number refer to different junctions on a given sample. All resistance values acquired after 15 h at 20 °C annealing, in the voltage range of ± 50 mV. [b] Not included in averages.

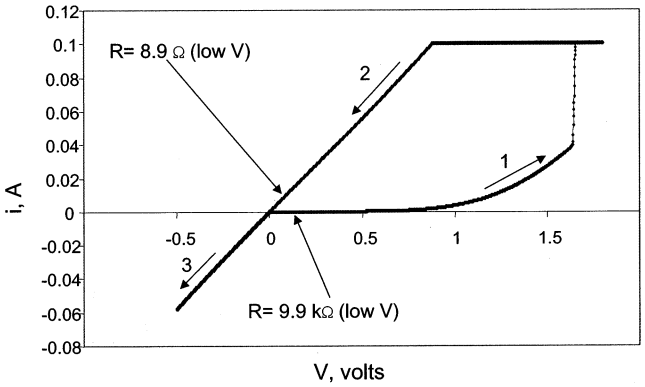

Figure 2. Current/voltage curve for a biphenyl junction scanned at 0.2 V/s at 20 °C. Positive voltage corresponds to the PPF being positive relative to Hg.

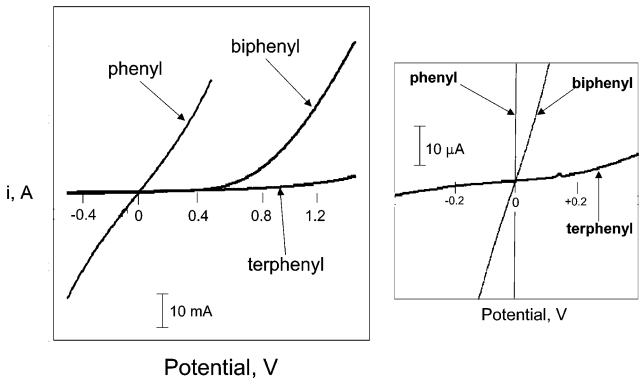

Figure 3. *i*/*V* curves for phenyl, biphenyl, and terphenyl at 20 °C. Inset shows expanded scale near the origin.

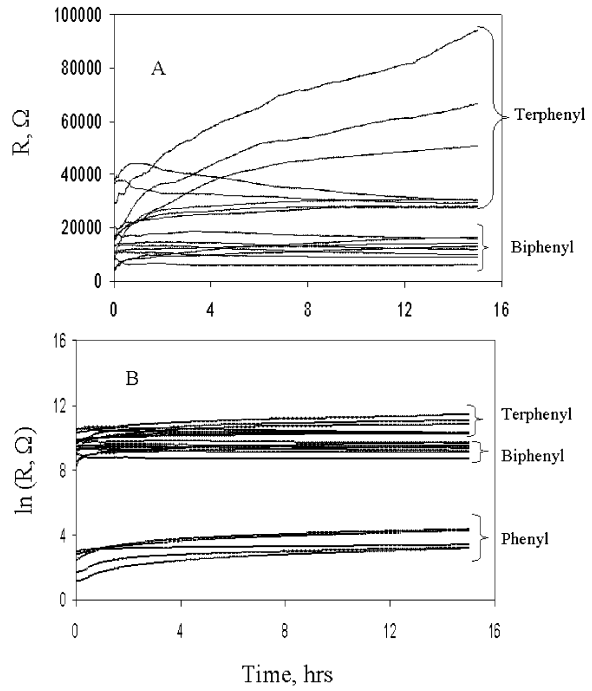

Figure 4. Observed behavior of junction resistance for $V = 0.05$ V for several phenyl, biphenyl, and terphenyl junctions as a function of time after junction formation. Temperature controlled at 20 °C. Upper plot shows eight biphenyl and eight terphenyl junctions on linear resistance scale, lower plot shows all three junction types on a log scale.

breakdown. All show a linear region at low potential (±100 mV), and all are nonlinear at higher voltage. The magnitude of the observed current and the observed junction resistance are strongly dependent on the length of the monolayer molecule. As shown in Table 2, there is significant variation in the observed low-voltage resistances for different samples and different spots on the same sample, presumably due to dust particles, residual electrolyte, or defects in the PPF or monolayers. The values indicated in the table were rejected as discordant, and the remaining values were averaged. The means and standard deviations of the remaining spots were 34.4 ± 19 Ω for phenyl, 13800 ± 6200 Ω for biphenyl, and 41000 ± 23900 Ω for terphenyl. Variations in the low voltage resistance with time after junction formation are shown in Figure 4. Although the terphenyl junctions show changes with time, they have consistently higher resistance than biphenyl junctions (Figure 4A). All three junction types are plotted in Figure 4B, on a log scale to permit comparison with the much more conductive phenyl junctions. As noted in the Discussion section,

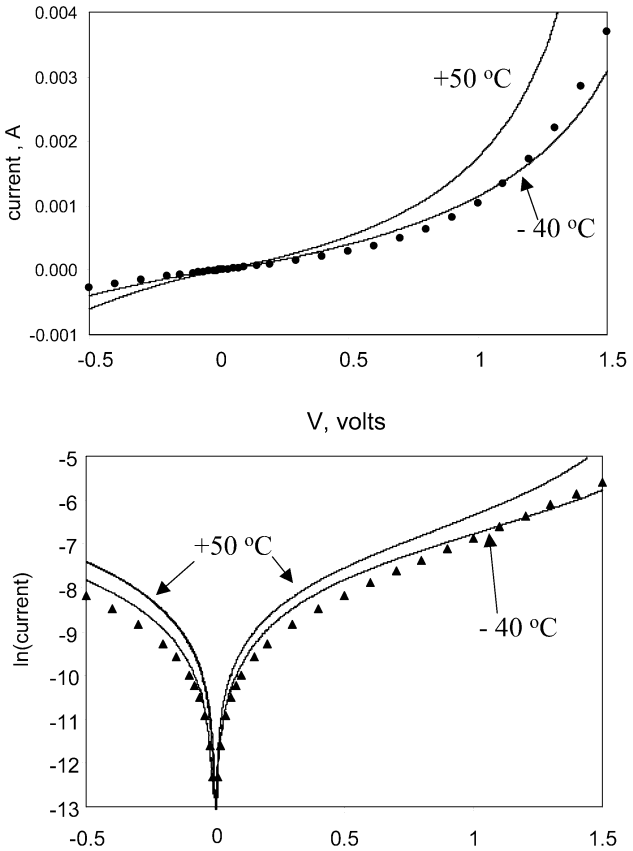

Figure 5. Current/voltage curves for a terphenyl junction at +50 and −40 °C. Solid lines are experimental, points were calculated from eq 1.

some of the variation in observed resistance with time and junction number may be due to impurities or defects, but it is important to note that the effect of molecular length is much larger than the variations apparent in Figure 4.

The shapes of the *i*/*V* curves in Figure 3 and the low voltage resistances listed in Table 2 provide tests of which conduction mechanisms apply to the phenyl, biphenyl, and terphenyl molecular junctions. For example, nonresonant coherent tunneling which fits the Simmons model is dictated by eq 1, with a strong dependence on monolayer thickness, but negligible temperature dependence.[39,40] Additional terms in eq 2 correspond to nonlinearity at high *V*.

$$j_T = V\frac{q^2(2m\Phi_T)^{1/2}}{h^2 d}\exp\left[\frac{-4\pi(2m\Phi_T)^{1/2}d}{h}\right] + \ldots \qquad (1)$$

where j_T = tunneling current density, m = electron mass, Φ_T = tunneling barrier, and h = Planck's constant. In contrast to coherent tunneling, thermionic emission and "hopping" have a much weaker thickness dependence but are exponentially dependent on temperature.

As summarized in Table 1, tunneling through a rectangular Simmons barrier is linear with *V* at low voltage and increases nonlinearly at higher *V*. Figure 5 shows attempts to fit the Simmons model to the *i*/*V* characteristic for terphenyl at −40 °C and +50 °C. The points shown in Figure 5 were calculated with the nonlinear Simmons equation including terms for both *V* and $V^{1/2}$, and are plotted on both a linear (circles) and logarithmic (triangles) current scale. For the −40 °C data set, eq 1 provides a close but not exact fit for terphenyl corresponding to a tunneling barrier of 2.55 eV and thickness of 15.1 Å.

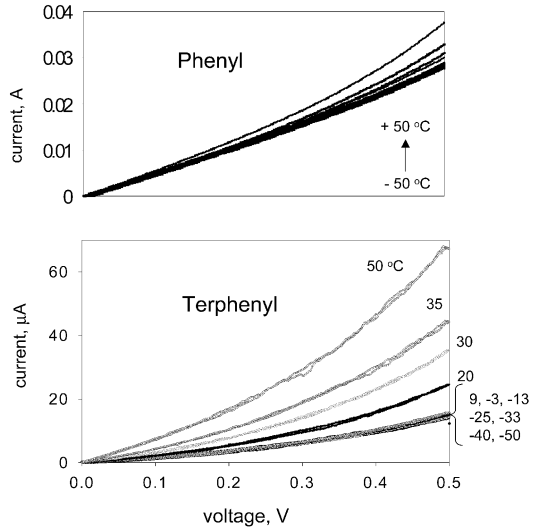

Figure 6. *i*/*V* curves for phenyl and terphenyl junctions with varying temperature. Recorded from the higher to lower temperatures shown, but changes with temperature were reversible.

Similar fits to the low-temperature *i*/*V* curves for phenyl and biphenyl yield Simmons barriers of 10 and 4.8 eV, respectively, assuming monolayer thicknesses of 6.6 and 11.1 Å. The inadequate fits of eq 1 and the variable barrier height with monolayer thickness indicate that the Simmons tunneling model does not explain the observations for the phenyl, biphenyl, and terphenyl homologous series. Furthermore, any tunneling process should have a weak temperature dependence, in conflict with the curves shown in Figure 5.

The effect of temperature on the *i*/*V* behavior of phenyl and terphenyl junctions is shown in more detail in Figure 6. The current for the phenyl junction depends weakly on temperature over the range of −50 to +50 °C, increasing by only 34% at a voltage of 0.5 V, and 17% at 0.1 V. The terphenyl junction, however, is essentially independent of temperature from −50 °C to +9 °C, increasing by only 3% at 0.5 V, but strongly temperature dependent between +9 °C and +50 °C, increasing 280% at 0.5 V. For a slightly higher temperature range, a different terphenyl junction showed an increase in current by a factor of 12 between 30 and 80 °C for $V = 0.5$ V, and a factor of 5.7 at $V = 0.05$ V. Observed currents for several temperatures and potentials are listed in Table 3 for a terphenyl junction. The data in Table 3 were obtained for a single junction cycled over a +50 to −50 °C temperature range.

As noted in Table 1, several conduction mechanisms are predicted to exhibit an exponential dependence on 1/*T*, since they involve thermal activation over an energy barrier. A plot of ln(*i*) vs 1/*T* is shown in Figure 7 for terphenyl at three voltages. The plot is linear for temperatures above 10 °C, with a slope of −3272 K at V = +0.5 V, −3568 K at V = 0.2 V, and −3629 K for V = 0.1 V. These slopes may be converted to eV by multiplying by *k*/*q*, yielding 0.28, 0.30, and 0.31 eV, respectively. The temperature dependence of the current for terphenyl above 10 °C indicates an activation barrier of 0.30 eV, which is independent of voltage over the range 0.05 to 0.5 V. Below 0 °C, the current through a terphenyl junction is independent of temperature, indicating that conduction occurs by a process which is not thermally activated.

Figure 8 shows additional ln i vs 1/*T* results for phenyl, biphenyl, and nitroazobenzene junctions, plotted on the same scale as terphenyl. Although NAB differs structurally from the phenylene series, it is included here because both 30 and 47 Å films show the distinct change in slope observed for terphenyl. The slopes of these plots are summarized in Table 4. All five junctions show a weak or negligible temperature dependence below 0 °C, with an apparent activation energy of <0.05 eV. Above 10 °C, the phenyl and biphenyl junctions continue to be independent of temperature, with a very slight or negligible increase in slope. The thicker junctions made from terphenyl and nitroazobenzene all show a significant barrier for the 10° to 50 °C temperature range. The observed slope varies somewhat for different junctions, within the range shown in Table 4. The slope for NAB varies with applied potential, with higher apparent activation barriers for lower applied potential. For example, the 47 Å NAB film exhibits a barrier of 0.85 eV from a ln(*i*) vs 1/*T* plot at $V = 50$ mV, but 0.51 eV for $V = 500$ mV. The significance of this variation is not yet known, but it is incorporated in the ranges listed in Table 4.

Discussion

The closest analogue to the current molecular junctions in the literature involves SAMs between a Hg drop and a solid metal or a second Hg drop.[14,15,20] The current densities observed here are significantly higher, although direct comparison is difficult due to differences in conditions and molecular structure. For example, the current density for the terphenyl monolayer listed in Table 3 at 20 °C and 0.5 V is 3×10^{-3} A/cm^2, while that observed for a junction between Ag/terphenyl thiol and Hg/$C_{16}H_{33}$thiol was 3×10^{-6} A/cm^2.[14] A junction formed between two Hg drops coated with a $C_{12}H_{25}S$ monolayer showed an approximate current density of 3×10^{-5} A/cm^2 at 0.5 V.[15] The shorter molecules and stronger molecule−substrate coupling in the current junctions may explain the higher current observed densities, but it would be premature to make significant conclusions solely on the basis of current density.

A pragmatic question about the current work regards the accuracy of Figure 1 as a representation of the junctions examined experimentally. On the basis of experience with SAMs in electrochemical and molecular electronic structures, defects and pinholes may be present which provide a low-resistance current path.[17] We have established previously that covalent monolayers deposited on glassy carbon and PPF are very low in pinholes, as judged by the inhibition of electron transfer to electrocatalytic redox systems such as dopamine.[31,41] The low pinhole density presumably results from the electrochemical derivatization by diazonium ion reduction. Pinholes would naturally be sites for more favorable reduction kinetics, which in turn generate additional phenyl radicals which chemisorb to the PPF. So pinholes which support electron transfer are inherently "self healing". It should also be noted that the C−C bond between the monolayer and the PPF substrate is formed irreversibly, so pinholes will not be created after monolayer deposition, at least by spontaneous desorption. In fact, nitrophenyl monolayers are stable to at least 400 °C in a vacuum, indicating their high stability.[42] A second argument against the involvement of pinholes in observed *i*/*V* curves is the strong dependence of current on molecular length and structure. Addition of one phenyl ring to the phenyl monolayer to yield biphenyl causes a resistance increase of a factor of 400. If junction conductivity resulted from a few pinholes, such a large change in resistance would not be expected. In addition, a 30 Å film of NAB has a resistance comparable to that of an 11 Å biphenyl monolayer below room temperature. On the basis of a recent report comparing conduction through conjugated stilbene oligomers to that in phenyl ethynyl oligomers,[21] the extensive conjugation of the NAB film would be expected to yield higher conductivity. In the current case, the high conduc-

TABLE 3: Current for Terphenyl Molecular Junction

potential, V	*i*, −50 °C, μamp	*i*, −40 °C, μamp	*i*, −33 °C, μamp	*i*, −25 °C, μamp	*i*, −13 °C, μamp	*i*, −03 °C, μamp	*i*, 09 °C, μamp	i, 20 °C, μamp	*i*, 30 °C, μamp	*i*, 35 °C, μamp	*i*, 50 °C, μamp
0.010	0.16	−0.06	0.22	0.23	0.07	−0.04	0.17	0.29	0.21	0.29	0.51
0.050	0.63	0.40	0.71	0.73	0.63	0.45	0.73	1.05	1.3	1.95	3.28
0.100	1.33	1.17	1.38	1.42	1.42	1.18	1.40	2.23	2.99	4.26	7.13
0.200	3.32	3.18	3.44	3.43	3.51	3.07	3.34	5.36	7.59	10.39	16.33
0.300	6.08	5.84	6.05	6.24	6.38	6.07	6.56	9.61	13.97	18.73	27.39
0.400	9.50	9.35	9.77	9.61	10.01	9.53	10.22	15.84	22.9	29.21	46.67
0.500	14.26	14.11	14.53	14.23	15.06	14.71	15.67	24.63	35.48	44.25	67.31

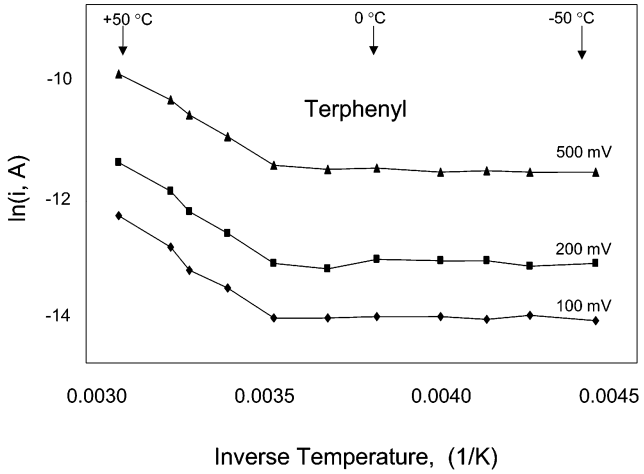

Figure 7. Plots of the terphenyl data from Figure 6 as ln(*i*) vs 1/*T* for three applied voltages.

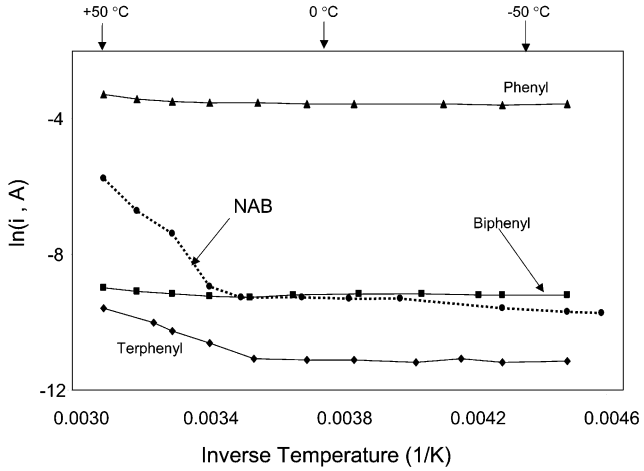

Figure 8. Comparison of temperature effects on phenyl, biphenyl, terphenyl, and nitroazobenzene (30 Å) junctions. Current was measured at +500 mV in all cases.

TABLE 4: Slopes of ln(*i*) vs 1/*T* Plots

molecule	layer thickness, Å	slope, eV, (+5 to +50 °C) $V = 0.5$ V	slope, eV (0 to −50 °C) $V = 0.5$ V
phenyl	6.6	<0.05	<0.02
biphenyl	11.1	<0.12	<0.02
terphenyl	15.1	0.28−0.31	<0.02
NAB	30 Å	0.62−0.76	<0.05
NAB	47 Å	0.4−0.85	<0.05

tivity of NAB overcomes its greater thickness, resulting in a lower resistance than terphenyl and comparable to biphenyl.

The nature of the monolayer/substrate bond is structurally well understood, based on XPS, AFM, Raman spectroscopy, etc. On glassy carbon, diazonium reduction yields monolayers having coverage equal to the theoretical close-packed values, and similar coverage has been observed on PPF.[36,43,44] Close packing would require that the phenyl rings of adjacent molecules are parallel, presumably forming domains of oriented phenyl rings. Since both GC and PPF are disordered, it is difficult to estimate the extent of possible monolayer ordering. GC20 has graphitic ribbons with widths of ∼50 Å, so it is unlikely that the monolayer can order over distances greater than 50 Å. For the edge of highly ordered pyrolytic graphite (HOPG), polarized Raman spectroscopy revealed that the NAB−graphite bond was rotated randomly, such that the surface bonding phenyl ring in NAB was rotationally disordered relative to the graphite planes.[45]

Although the Hg/monolayer contact was formed quickly after monolayer deposition, brief exposure to air was likely to create a layer of adsorbed impurities on the Hg or monolayer, or both. However, such impurities should affect all junctions listed in Table 2 similarly, since the monolayer/Hg contact is formed identically for all molecules of different lengths. The strong dependence of resistance on length, and the negligible resistance observed in the absence of a monolayer, rule out a significant effect of impurities on the results. From Table 2, it is apparent that the average biphenyl junction resistance is 400 times that of a phenyl junction, and the terphenyl junction resistance is 1200 times that of a phenyl junction, despite the fact that their monolayer/carbon and monolayer/Hg interfaces are identical. An additional issue is the flatness of the PPF relative to the monolayer thickness. AFM shows that PPF has an RMS roughness of <5 Å, and the peaks and valleys are quite gradual.[36] The liquid Hg contact presumably conforms to some of these height variations, but to what degree is unknown. At present, there is significant uncertainty in the functional contact area between Hg and the top of the monolayer. The geometric area of 0.8 mm^2 sets an upper limit, but a combination of surface height variation and impurities may result in a smaller effective area.

The apparent breakdown voltages such as that shown in Figure 2 did not vary systematically with layer thickness, presumably due to the strong influence of defects on breakdown. For biphenyl and terphenyl, breakdown occurred in the range of 0.8 to 1.6 V, while breakdown for phenyl was not observed before the current exceeded the 100 mA limit of the instrument. The observed range of breakdown fields was 4−14 MV/cm for biphenyl and terphenyl, and in all cases breakdown was irreversible. Breakdown fields for junctions between two SAMs have been reported as 2-5.3 MV/cm, and a thioterphenyl/$C_{16}H_{35}$-SH junction yielded 4.9 MV/cm.[14] Reported breakdown fields for dielectric materials range (at least) from 0.03 MV/cm for air and 0.4 MV/cm for vacuum to 10 MV/cm for poly(methyl methacrylate) and 10−20 MV/cm for SiO_2 thin films.[46,47] The observation that the carbon-based biphenyl and terphenyl junctions exhibit breakdown fields comparable to other molecular junctions and to conventional dielectric materials further supports the conclusion that the current junctions are low in pinholes.

The invariance of the voltammograms shown in Figure 3 with scan rate and the lack of significant hysteresis upon scan reversal are not surprising for a molecular junction, but they do rule out any mass transport effects such as would be expected for voltammetry of solutions or solid electrolytes.[28] This observation reinforces the fact that molecular junctions differ fundamentally from electrochemical interfaces, since there is neither solvation nor counterions to neutralize local charges. Since the junctions are structurally asymmetric, some rectification is expected, due to differences in work functions between PPF and Hg, and to the existence of the monolayer/PPF covalent bond. The observed ratio of forward to reverse current at a given bias was in the range of 0.8 to 2.0 for voltages below 0.5 V. This asymmetry is small compared to molecular and semiconductor rectifiers, and presumably results from either the PPF/monolayer or monolayer/Hg junctions.

The most important observation from the current results is the change from temperature-dependent *i*/*V* characteristics above about 5 °C to temperature-independent curves below 5 °C. This fact rules out temperature-dependent conduction mechanisms such as those listed in Table 2, and leaves only tunneling at low temperatures. Stated differently, conduction becomes adiabatic at low temperature, but a nonadiabatic process begins to operate as the temperature exceeds ∼5 °C. The low-temperature route cannot involve conventional Marcus or Butler−Volmer electron-transfer kinetics, as there can be no nuclear reorganization to lead to a transition state. The transition at ∼5 °C and the 0.3 eV activation barrier observed for terphenyl leads to the likely identity of the structural change associated with thermal activation. Suppose that the benzene rings in a given terphenyl molecule exist in a range of dihedral angles with respect to each other. Free biphenyl has a dihedral angle close to 30°, but a range of angles would be expected in a close-packed monolayer. Furthermore, suppose that one conformer of a terphenyl molecule is more conductive than others, presumably one with coplanar benzene rings. Calculated HOMO−LUMO gaps for terphenyl (Gaussian 98, B3LYP/6-31G(d)) are 4.28 eV for the planar molecule and 4.75 for the minimum energy twisted form, hence the higher conductivity expected for the planar form. Given that a nonplanar terphenyl is energetically more favorable, the planar molecule would be expected to be a minority conformer. When the junction is cooled, ring rotation would freeze out and some terphenyl molecules will exist in the coplanar conformer. Once the monolayer is frozen below 5 °C, further cooling has little effect on junction conductance, as the distribution of rotamers remains constant.

As the temperature increases above 5 °C, rotational motion occurs and additional molecules may transiently exist in the coplanar conformation. Rotational motion is governed by an Arrhenius relationship, hence the linear dependence of ln(*i*) on 1/*T*. The 0.28−0.31 eV slope observed for terphenyl corresponds to the activation barrier for phenyl ring rotation in the junction monolayer, and is equivalent to the reorganization energy in conventional nonadiadatic electron transfer. Reported values for phenyl ring rotation depend on substituents, but range from ∼0.1 eV for unsubstituted biphenyl to 0.2 eV for terphenyl lacking ortho substituents.[48−50] Polyphenylene oligomers may be better analogues to a closed packed monolayer, and methyl-substituted polyphenylenes exhibit a rotational barrier of 0.7 to 0.8 eV.[51] Therefore, the 0.3 eV barrier observed for terphenyl junctions is within the range expected for phenyl ring rotation.

Figure 9 shows the predicted behavior of the proposed mechanism as a function of monolayer thickness. The fraction

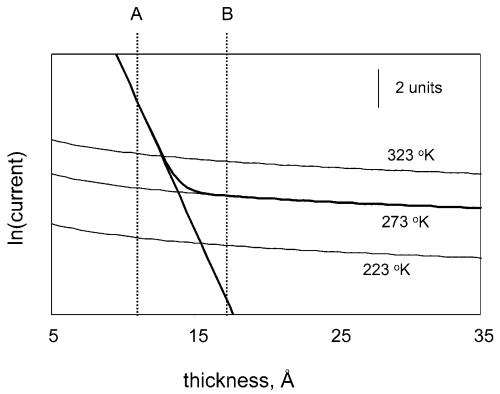

Figure 9. Calculated dependence of current on monolayer thickness for a combination of tunneling and a thermally activated conduction mechanisms. Diagonal straight line was calculated for coherent tunneling with an exponential thickness dependence; the three curves were calculated for an activated process with a 0.3 eV barrier. A and B indicate molecular lengths in the tunneling and thermal limits, respectively. Absolute current scale and intersection points depend on the fraction of active molecules and the tunneling and thermal barrier heights.

of molecules in the planar conformation in the frozen monolayers determines the absolute *y*-axis scale, and the tunneling barrier determines the slope of the tunneling contribution. Although these parameters are unknown, Figure 9 illustrates the trends expected with molecule length and temperature based on a 0.3 eV activation barrier. As the molecule becomes shorter, tunneling becomes more probable until it exceeds the thermal process. A molecule of length "A" in Figure 9 will exhibit a temperature-independent conductivity, as tunneling is the dominant conduction mechanism. A molecule with length "B" is controlled by the thermal process, as tunneling is too slow. Case A appears to apply to the phenyl and biphenyl monolayers, leading to the behavior apparent in Figure 8. At sufficiently high temperatures, biphenyl and phenyl junctions are predicted to become temperature dependent, as rotational motion leads to a larger fraction of molecules in the planar conformation.

Given that the low-temperature conductivity of all molecules studied here indicates conduction by tunneling, the nature of the tunneling process should be considered. The Simmons model has been rejected for numerous examples in electrochemistry and molecular electronics, in favor of alternatives which take molecular structure into account.[1,14,27,52] The sequence of phenyl, biphenyl, and terphenyl is too short to reliably test the distance dependence, but it is clear that the conjugation of the monolayer molecule has a significant effect on junction resistance. A likely possibility is the "tight binding" or "incoherent" model in which electron conduction occurs by a series of tunneling steps between "sites", possibly phenyl rings in the current junctions.[27] Conjugation in NAB and coplanarity in terphenyl should increase the electronic coupling between sites, and increase the tunneling probability.[53]

An additional important implication of the low temperature data regards the nature of the monolayer−PPF contact. The linearity of the *i*/*V* curves at low temperature and voltage is not expected for a contact involving a Schottky barrier, and implies an essentially ohmic contact. Au/thiol SAMs often show a large onset potential of 0.7−2 V, usually attributed to energy mismatch between the monolayer energy levels and the contact Fermi level.[3,12,25] For example, a "break junction" consisting of a few benzene 1,4-dithiolate molecules bridging a ∼9 Å gap between gold contacts exhibited a "Coulomb blockage gap" of 0.7 V before conduction occurred.[12] The apparent lack of an

onset potential in Figure 3 implies that any barrier in PPF/monolayer/Hg is smaller than kT (19 meV at 223 °K). It is too early to conclude definitively, but it is possible that the symmetric phenyl−phenyl linkage between the graphitic PPF and the organic monolayer reduces such barriers to small values, and the PPF/molecule junction approaches the behavior of an ohmic contact.

Finally, a comparison of the molecular junction of Figure 1 to reported alternatives is useful, with respect to "molecular resistance". Several determinations have been reported for the resistance of a single molecule, ranging over a wide range between <1 MΩ and >10 GΩ.[3,8,11,12,22,23,54] Based on a coverage of 5×10^{-10} mol/cm^2, the junctions examined here consist of $\sim 10^{12}$ molecules arranged in parallel. If all molecules in a terphenyl junction with 41 KΩ observed resistance behaved identically, a single molecule resistance of 10^{16} ohms is predicted. While this value is unexpectedly high, it is lower than that calculated from the current densities for Hg/SAM junctions discussed earlier.[14,15,20] Cui et al.[54] reported a resistance of 900 ± 50 MΩ for an octanedithiol molecule, but noted that the resistance was about 4 orders of magnitude higher when a nonbonding contact was made to the molecule. The large discrepancy between reported single molecule resistances and the apparent values observed here could be caused by several factors, including the minority population of conductive molecules, a small effective junction area or increased thickness due to impurities, a nonbonding molecule−mercury contact or lateral interactions within the monolayer which prevent the molecules from acting independently. Dilution experiments and much smaller junctions are currently under investigation to understand the apparent failure of scaling relations.

Acknowledgment. This work was supported by the Analytical and Surface Chemistry Division of the National Science Foundation, through Grant 9819978. The authors acknowledge productive conversations with Mark Ratner, Clifford Kubiak, and John Swenton during the course of this work.

References and Notes

(1) Jortner, J.; Ratner, M. *Molecular Electronics*; Blackwell Science Ltd.: Cambridge, MA, 1997.
(2) Mirkin, C. A.; Ratner, M. A. *Annu. Rev. Phys. Chem.* **1992**, *43*, 719.
(3) Datta, S.; Tian, W.; Hong, S.; Reifenberger, R.; Henderson, J. I.; Kubiak, C. P. *Phys. Rev. Lett.* **1997**, *79*, 2530.
(4) Feldheim, D. L.; Grabar, K. C.; Natan, M. J.; Mallouk, T. E. *J. Am. Chem. Soc.* **1996**, *118*, 7640.
(5) Brousseau, L. C.; Zhao, Q.; Shultz, D. A.; Feldheim, D. L. *J. Am. Chem. Soc.* **1998**, *120*, 7645.
(6) Zhou, C.; Deshpande, M. R.; Reed, M. A.; Jones, L.; Tour, J. M. *Appl. Phys. Lett.* **1997**, *71*, 661.
(7) Tian, W.; Datta, S.; Hong, S.; Reifenberger, R.; Henderson, J. I.; Kubiak, C. P. *J. Chem. Phys.* **1998**, *109*, 2874.
(8) Chen, J.; Calvet, L. C.; Reed, M. A.; Carr, D. W.; Grubisha, D. S.; Bennett, D. W. *Chem. Phys. Lett.* **1999**, *313*, 741.
(9) Metzger, R. M.; Chen, B.; Hopfner, U.; Lakshmikantham, M. V.; Vuillame, D.; Kawai, T.; Wu, X.; Tachibana, H.; Hughes, T. V.; Sakurai, H.; Baldwin, J. W.; Hosch, C.; Cava, M. P.; Brehmer, L.; Ashwell, G. J. *J. Am. Chem. Soc.* **1997**, *119*, 10455.
(10) Gittins, D. I.; Bethell, D.; Schiffrin, D. J.; Nichols, R. J. *Nature* **2000**, *408*, 67.
(11) Kergueris, C.; Bourgoin, J. P.; Palacin, S.; Esteve, D.; Urbina, C.; Magoga, M.; Joachim, C. *Phys. Rev. B* **1999**, *59*, 12505.
(12) Reed, M. A.; Zhou, C.; Muller, C. J.; Burgin, T. P.; Tour, J. M. *Science* **1997**, *278*, 252.
(13) Schon, J. H.; Meng, H.; Bao, Z. *Science* **2001**, *294*, 2138.
(14) Holmlin, R. E.; Haag, R.; Chabinyc, M. L.; Ismagilov, R. F.; Cohen, A. E.; Terfort, A.; Rampi, M. A.; Whitesides, G. M. *J. Am. Chem. Soc.* **2001**, *123*, 5075.
(15) Slowinski, K.; Majda, M. *J. Elect. Chem.* **2000**, *491*, 139.
(16) Ranganathan, S.; Steidel, I.; Anariba, F.; McCreery, R. L. *Nano Lett.* **2001**, *1*, 491.
(17) Finklea, H. O. Electrochemistry of Organized Monolayers of Thiols and Related Molecules on Electrodes. In *Electroanalytical Chemistry*; Bard, A. J., Ed.; Dekker: NewYork, 1996; Vol. 19, p 109.
(18) Smalley, J. F.; Feldberg, S. W.; Chidsey, C. E. D.; Linford, M. R.; Newton, M. D.; Liu, Y.-P. *J. Phys. Chem.* **1995**, *99*, 13141.
(19) Sachs, S. B.; Dudek, S. P.; Hsung, R. P.; Sita, L. R.; Smalley, J. F.; Newton, M. D.; Feldberg, S. W.; Chidsey, C. E. D. *J. Am. Chem. Soc.* **1997**, *119*, 10563.
(20) Slowinski, K.; Chamberlain, R. V.; Miller, C. J.; Majda, M. *J. Am. Chem. Soc.* **1997**, *119*, 11910.
(21) Sikes, H. D.; Smalley, J. F.; Dudek, S. P.; Cook, A. R.; Newton, M. D.; Chidsey, C. E. D.; Feldberg, S. W. *Science (Washington, DC)* **2001**, *291*, 1519.
(22) Collier, C. P.; Wong, E. W.; Belohradsky, M.; Raymo, F. M.; Stoddart, J. F.; Kuekes, P. J.; Williams, R. S.; Heath, J. R. *Science* **1999**, *285*, 391.
(23) Collier, C. P.; Mattersteig, G.; Wong, E. W.; Luo, Y.; Beverly, K.; Sampaio, J.; Raymo, F. M.; Stoddart, J. F.; Heath, J. R. *Science* **2000**, *289*, 1172.
(24) Bumm, L. A.; Arnold, J. J.; Dunbar, T. D.; Allara, D. L.; Weiss, P. S. *J. Phys. Chem.* **1999**, *103*, 8122.
(25) Hong, S.; Reifenberger, R.; Tian, W.; Datta, S.; Henderson, J.; Kubiak, C. P. *Superlattices Microstruct.* **2000**, *28*, 289.
(26) Fan, F.-R. F.; Yang, J.; Dirk, S. M.; Price, D. W.; Kosynkin, D.; Tour, J. M.; Bard, A. J. *J. Am. Chem. Soc. B* 2001.
(27) Mujica, V.; Ratner, M. A. *Chem. Phys.* **2001**, *264*, 365.
(28) Terrill, R. H.; Murray, R. W. Electron Hopping Transport in Electrochemically Active, Molecular Mixed Valent Materials. In *Molecular Electronics*; Jortner, J., Ratner, M., Eds.; Blackwell Science Ltd.: Cambridge, MA, 1997; p 215.
(29) Bixon, M.; Jortner, J. *J. Am. Chem. Soc.* **2001**, *123*, 12556.
(30) Bixon, M.; Jortner, J. *J. Phys. Chem. A* **2001**, *105*, 10322.
(31) DuVall, S.; McCreery, R. L. *J. Am. Chem. Soc.* **2000**, *122*, 6759.
(32) Yang, H.-H.; McCreery, R. L. *J. Electrochem. Soc.* **2000**, *147*, 3420.
(33) Allongue, P.; Delamar, M.; Desbat, B.; Fagebaume, O.; Hitmi, R.; Pinson, J.; Saveant, J. M. *J. Am. Chem. Soc.* **1997**, *119*, 201.
(34) Delamar, M.; Hitmi, R.; Pinson, J.; Saveant, J. M. *J. Am. Chem. Soc.* **1992**, *114*, 5883.
(35) Ranganathan, S.; McCreery, R. L.; Majji, S. M.; Madou, M. *J. Electrochem. Soc.* **2000**, *147*, 277.
(36) Ranganathan, S.; McCreery, R. L. *Anal. Chem.* **2001**, *73*, 893.
(37) Ranganathan, S.; Kuo, T.-C.; McCreery, R. L. *Anal. Chem.* **1999**, *71*, 3574.
(38) Ranganathan, S. Preparation, Modification and Characterization of a Novel Carbon Electrode Material for Applications in Electrochemistry and Molecular Electronics. Ph.D. Thesis, The Ohio State University, 2001.
(39) Lamb, D. R. *Electrical Conduction Mechanisms in Thin Insulating Films*; Methuen and Co.: London, 1968.
(40) Simmons, J. G. *DC Conduction in Thin Films*; Mills and Boon Limited: London, 1971.
(41) DuVall, S.; McCreery, R. L. *Anal. Chem.* **1999**, *71*, 4594.
(42) Kuo, T.-C. Raman Spectroscopy and Electrochemistry of Modified Carbon Surfaces. Ph.D. Thesis, The Ohio State University, 1999.
(43) Liu, Y.-C.; McCreery, R. L. *J. Am. Chem. Soc.* **1995**, *117*, 11254.
(44) McCreery, R. L. Carbon Electrodes: Structural Effects on Electron-Transfer Kinetics. In *Electroanalytical Chemistry*; Bard, A. J., Ed.; Dekker: New York, 1991; Vol. 17, p 221.
(45) Liu, Y.-C.; McCreery, R. L. *Anal. Chem.* **1997**, *69*, 2091.
(46) O'Dwyer, J. J. *Theory of Electrical Conduction and Breakdown in Solid Dielectrics*; Clarendon Press: Oxford, England, 1973.
(47) Gallagher, T. J.; Pearmain, A. J. *High Voltage Testing and Design*; John Wiley & Sons: New York, 1983.
(48) Eliel, E.; Wilen, S. *Stereochemistry of Organic Compounds*; John Wiley and Sons: New York, 1996.
(49) Melzer, P.; Kurreck, H.; Kieslich, W. *Fed. Rep. Ger. Chem. Ber.* **1982**, *115*, 3597.
(50) Goller, A.; Grummt, U.-W. *Chem. Phys. Lett.* **2000**, *321*, 399.
(51) Pasco, S. T.; Baker, G. L. *Synth. Met.* **1997**, *84*, 275.
(52) Yaliraki, S. N.; Roitberg, A. E.; Gonzalez, C.; Mujica, V.; Ratner, M. A. *J. Phys. Chem.* **1999**, *111*, 6997.
(53) Holten, D.; Bocian, D. F.; Lindsey, J. S. *Acc. Chem. Res.* **2002**, *35*, 57.
(54) Cui, X. D.; Primak, A.; Zarate, X.; Tomfohr, J.; Sankey, O. F.; Moore, A. L.; Moore, T. A.; Gust, D.; Harris, G.; Lindsay, S. M. *Science* **2001**, *294*, 571.
(55) Sze, S. M. *The Physics of Semiconductor Devices*, 2nd ed.; Wiley: New York, 1981.
(56) Burin, A. L.; Ratner, M. A. *J. Phys. Chem.* **2000**, *113*, 3941.